Meta Gene 20 (2019) 100553

Contents lists available at ScienceDirect

Meta Gene

journal homepage: www.elsevier.com/locate/mgene

Liraglutide alters hepatic metabolism in high-fat fed obese mice: A bioinformatic prediction and functional analysis

Isabelle Arruda Barbosa[a,1], Eloá Mangabeira Santos[a,1], Alanna Fernandes Paraíso[a,b], Pablo Vinicyus Ferreira Chagas[a], Luís Paulo Oliveira[a], João Marcus Oliveira Andrade[a,b], Lucyana Conceição Farias[a], Bruna Mara Aparecida de Carvalho[c], Alfredo Maurício Batista de Paula[a], André Luiz Sena Guimarães[a], Sérgio Henrique Sousa Santos[a,c,*]

[a] Laboratory of Health Science, Postgraduate Program in Health Science, Universidade Estadual de Montes Claros (Unimontes), Montes Claros, Minas Gerais, Brazil
[b] Faculdades Santo Agostinho, Montes Claros, Minas Gerais, Brazil
[c] Institute of Agricultural Sciences (ICA), Food Engineering, Universidade Federal de Minas Gerais (UFMG), Montes Claros, Minas Gerais, Brazil.

ARTICLE INFO

Keywords:
Hepatic steatosis
Metabolic syndrome
Obesity
Leader gene

ABSTRACT

Liraglutide, an important pharmacological agent used to improve glycemic status and weight control, has emerged as a therapeutic strategy for hepatic steatosis treatment.

Objective: The aim of the present study was to analyze the influence of liraglutide in hepatic steatosis and evaluate the potential target genes involved in the liraglutide action in the hepatic steatosis through a bioinformatics study.

Methods & procedures: We performed an animal study with male mice divided into three groups: standard, high-fat diet and the third group were fed a high-fat diet and treated with liraglutide at a dose of 0.6 mg/kg body weight. Blood parameters (glucose tolerance and insulin sensitivity tests, total cholesterol, high-density lipoprotein-C, triglycerides and glucose levels) were evaluated. mRNA analysis for *ACC* and *FAS* were performed. Gene databases, and bioinformatics algorithms were used to generate molecular targets for liraglutide and hepatic steatosis based on in silico investigation. Interactions networks between protein coding were accessed.

Results: The present study showed that liraglutide decreased glucose levels, total cholesterol and triglycerides in obese animals as compared to the high-fat-fed obese mice. *AKT* and *RPS6KB1* genes presented higher disease-related connectivity. Interaction Network exhibited a power law behavior in correlation: 0.896; R2: 0.796. Ontological analysis demonstrated different mechanisms associated such as regulation of signaling process.

Conclusion: The present study reveals relevant information regarding the liraglutide effects in hepatic steatosis. The liraglutide improved hyperglycemia and attenuated hepatic steatosis in mice fed a high-fat diet.

1. Introduction

Non-alcoholic fatty liver disease (NAFLD), one of the most common liver disease in the world, refers to a spectrum of hepatic disorders responsible by an increase in hepatic triglyceride content (Cohen et al., 2011), being these alterations considered clinic/pathological components of the metabolic syndrome (MetS) that is associated with insulin resistance, obesity, hyperlipidemia, hypertension and type II diabetes (Fotbolcu and Zorlu, 2016; Bambha et al., 2012; Rector et al., 2008). NAFLD may be characterized by the presence of nonalcoholic steatohepatitis, liver cirrhosis and steatosis (Bambha et al., 2012; Rector et al., 2008; Targher et al., 2008).

Obesity is strongly associated with adiposity and metabolic dysfunction (Ng et al., 2010; Shepard et al., 2001; Cameron-Smith et al., 2003; Weisberg et al., 2006; Buettner et al., 2007), which can lead to the development of hepatic steatosis (Fotbolcu and Zorlu, 2016), caused by dysregulation of fatty acid metabolism, inducing triglycerides and liver free fatty acids increased levels. This state may contribute to augmented hepatocytes susceptibility to oxidative stress and inflammation. Up to date, therapeutic strategies for obesity and hepatic

* Corresponding author at: Institute of Agricultural Sciences. Food Engineering College, Universidade Federal de Minas Gerais (UFMG), Avenida Universitária, 1.000 – Universitário, 39, 404-547, Montes Claros, MG, Brazil.
E-mail address: sergiosantos@icb.ufmg.br (S.H.S. Santos).
[1] Equally contributed to this study.

https://doi.org/10.1016/j.mgene.2019.100553
Received 3 September 2018; Received in revised form 21 December 2018; Accepted 20 February 2019
Available online 22 February 2019

steatosis are still very limited (Stal, 2015; Ono et al., 2003). The current treatment for metabolic dysfunction is associated to lifestyle modifications and weight loss, being necessary the study of effective pharmacological treatments.

Glucagon-like peptide (GLP)-1 is an incretin hormone that has been shown to affect glucose, lipid and hepatic metabolism. Liraglutide, a GLP-1 analogue with 97% identity to the human GLP-1, is being currently used as a new therapy for glucose control (Kim and Egan, 2008; Lee et al., 2012). Liraglutide promotes the gastric emptying and reduces hunger, thereby reducing body weight and body fat mass (Bode, 2012; Scott, 2014). Recent studies with mice models have demonstrated the liraglutide effects in oxidative stress and inflammatory response in the liver (Gao et al., 2015). All these effects are mediated by the activation of GLP-1 (Fotbolcu and Zorlu, 2016).

In a recent study from Na and colls (Ao et al., 2016), treatment with GLP-1 attenuated lipids accumulation in the liver, reduced inflammation and improved metabolic parameters. Additionally, other study in obese mice showed that liraglutide treatment is capable of reducing lipid accumulation in the liver and insulin resistance (Gao et al., 2015; Mells et al., 2012).

However, the mechanisms by which liraglutide may reverse steatosis hepatic still remains obscure. Thus, bioinformatic analysis can be a useful tool to investigate new mechanisms action, as well as to identify the spectrum of biologic processes targeted by liraglutide. Bioinformatics is a promising and interesting tool that has been used to better understand molecular pathways of several pathologic processes, such as oral lichen planus, skin carcinoma, pressure ulcer, radicular cyst and periapical granuloma (Orlando et al., 2013; Poswar Fde et al., 2015; Santos et al., 2017; Poswar et al., 2017).

In the present study, we aimed to explore through functional assays and bioinformatic approach, the liraglutide role on hepatic steatosis in high-fat fed mice, and also the possible gene interactions network and molecular targets.

2. Material and methods

2.1. Experimental design

Male FVB/N mice (4 weeks old) kindly donated by the Universidade Federal de Minas Gerais (Belo Horizonte, Minas Gerais, Brazil) were used in this experiment. The mice were maintained under 12 h light/dark cycles at a temperature of 23.0 ± 2.0 °C with unlimited access to food and water. After an adaptation period, mice were randomly categorized into three groups (n = 7) and fed for 8 weeks with the following experimental diets: standard diet (ST), high-fat diet (HFD) and high-fat diet plus Liraglutide (HFD + LIR). After this period of obesity induction, the third group received daily subcutaneous injections of Liraglutide for 60 days at a dosage of 0.6 mg/kg body weight (Novo Nordisk, Brazil) (Gao et al., 2015).

The high-fat diet, composed of 24.55% carbohydrate, 14.47% protein and 60.98% fat, with a total of 5.28 kcal per 1 g of diet, was prepared according to the protocols previously reported. Standard diet (Purina – Labina®), which was used for the regular maintenance of our mice, was composed of 50.3% carbohydrate, 41.9% protein and 7.8% fat, with a total of 2.18 kcal per 1 g of diet. All of the high-fat diet components were purchased from Rhoster® LTDA (São Paulo, Brazil).

All animal experiments were in accordance with the Principles of Laboratory Animal Care and approved by the Animal Ethics Committee from Unimontes, Montes Claros, Brazil, by the process n°056 /2012.

2.2. Measurement of liver lipid content

One liver lobe was snap frozen, processed in a cryostat, and stained with Sudan Black, which is specific to stain for lipids. All slides were photographed on Brightfield microscope FSX100 (Olympus, Center Valley, PA, USA) at 20×.

2.3. Glucose tolerance and insulin sensitivity tests

Intraperitoneal glucose tolerance test (IPGTT) was conducted without anesthesia in the morning period. For the test, d–glucose (2 mg/g body weight) was administered in fasted mice by intraperitoneal injection. Blood samples were collected from the tail at 0, 15, 30, 60, and 120 min after injection, and glucose levels were measured. The insulin sensitivity test (IPIST) was performed on overnight-fed mice, after intraperitoneal injection of insulin (0.75 units/kg body weight, Sigma–Aldrich®, St. Louis, USA). Tail blood samples were taken at 0, 15, 30, and 60 min after injection. Blood glucose levels were determined using an Accu-Check Active glucometer (Roche Diagnostics ®, Indianapolis, USA).

2.4. Tissue collection, reverse transcription, and real-time PCR (qRT-PCR)

The mice were sacrificed by decapitation after 4 months of treatment. The liver was removed, weighed, immediately frozen in liquid nitrogen and stored at −80 °C for RNA extraction.

The liver tissue collected were homogenized and the total RNA was isolated using Trizol reagent (Invitrogen Corp. VR, San Diego, CA, USA) according to the protocol provided by the manufacturer. The total RNA was treated with DNAse. Reverse transcription was performed with M-MLV (Invitrogen Corp. VR) using random hexamer primers. Polymerase chain reaction for Acetyl-CoA carboxylase (*ACC*) and Fatty Acid Synthase (*FAS*) was performed in duplicate in a Real Time PCR on a Step One Plus equipment (Applied Biosystems). Real-time quantitative PCR was performed using Power SYBR Green (Applied Biosystems).

The sequences for the primers were: *GAPDH* (FW: 5′AACGACCCC TTCATTGACCTC 3′; RV: 5′ CTTCCCATTCTCAGCCTTGACT 3′) *ACC* (FW: 5′ GAACATCCCCACGCTAAACAGA 3′; RV: 5′ CTGACAAGGTGGC GTGAAGG 3′) and *FAS* (FW: 5′CATCCTAGGCATCCGAGACCT 3′; RV: 5′ ATCGTGTTCTCGTTCCAGGATC 3′). All samples were normalized to Glyceraldehyde-3-phosphate dehydrogenase (*GAPDH*), which served as an endogenous control. The relative comparative CT method of Livak and Schmittgen was applied to compare gene expression levels between groups. Normalization of the target genes to the reference gene was performed using the $2^{-\Delta\Delta CT}$ method, where $\Delta\Delta C_T = (C_{T,target} - C_{T,reference})$ treated sample $- (C_{T,target} - C_{T,reference})$ untreated sample (Livak and Schmittgen, 2001).

2.5. Determination of biochemical parameters

Blood samples were collected after sacrifice, centrifuged (3.200 rpm for 10 min at 4 °C) and the serum was separated (Centrifuga Excelsa II, Mod. 206 BL). Serum triglycerides, glucose, High-Density-Lipoprotein (HDL-c), total cholesterol, aspartate aminotransferase and alanine transaminase levels were measured using enzymatic tests (Wiener lab BT3000 analyzer, Argentina).

2.6. Histological analyses

The liver were excised and fixed in 4% buffered-formalin solution and embedded in paraffin. Sections were deparaffinized, rehydrated, and stained with hematoxylin and eosin. Microvesicular structures, characteristic of steatosis were evaluated under a conventional light microscope (Axioskop40). Images of liver areas (×10 ocular and ×40 objective lenses) were captured with an Axio Cam MRcZeis camera.

2.7. Bioinformatics analyses

Initially the keywords (Liraglutide, obesity, glycemia and steatosis) were stablished according to Medical Subject Headings (MeSH) (www.nlm.nih.gov/mesh). In a second step a literature review was performed to identify genes involved with the keywords chosen (Poswar et al., 2017). A search considering only human genes was performed on the

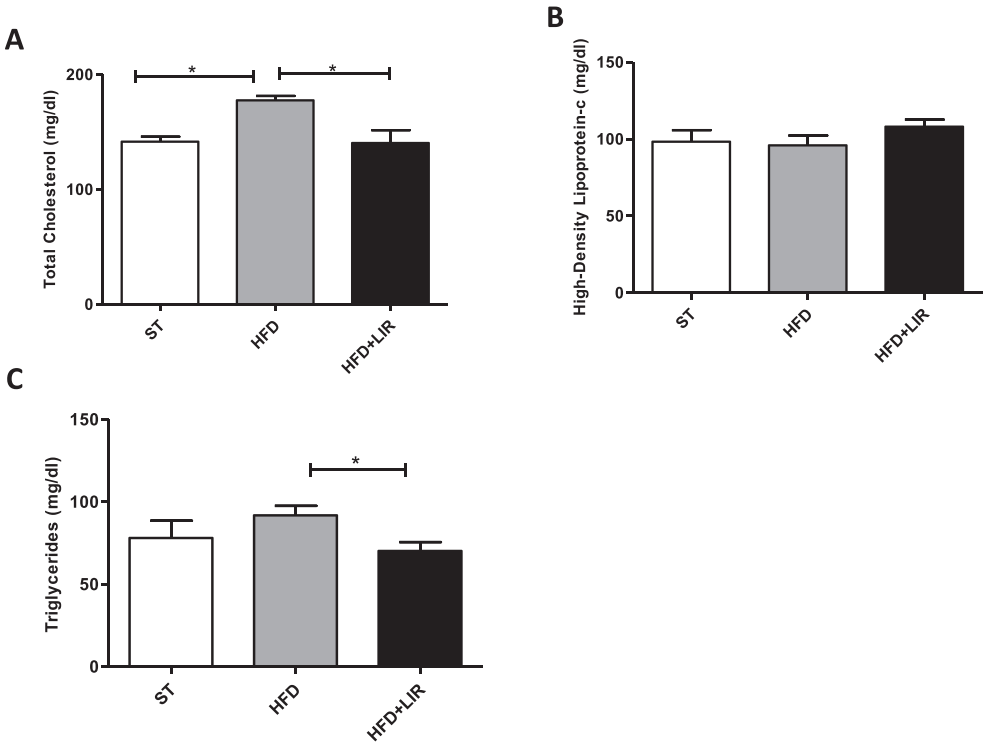

Fig. 1. Blood parameters of mice-fed standard (ST), high-fat diet (HFD), and HFD with liraglutide (HFD + LIR). (A) Total cholesterol (mg/dL) (B) High Density Lipoprotein-c (mg/dL) (C) Triglycerides (mg/dL). * $p < .05$; **$p < .01$ (one-way ANOVA).

following databases: NCBI, PubMed, and Genecards (Rebhan et al., 1997) to determine the primary set of genes (Poswar et al., 2017). The Human Genome Organization gene nomenclature was adopted (HUGO). After this step, lists of potential candidate genes related to the keywords were generated. The initial gene list was then expanded using the Web-available software STRING (version 10.0) and STITCH (version 5.0) (Santos et al., 2017; von Mering et al., 2005; Jensen et al., 2009). Only interactions based on experimental observations described in the public domain and available in specific databases were considered with a high degree of confidence (above 0.9, range 0–0.99) (Orlando et al., 2013; Covani et al., 2008; Bragazzi et al., 2011). Literature-based data from PubMed were used to avoid false positives in the data analysis. The STRING software was used to score each interaction and build maps among the identified genes. For each gene identified, we summed combined association scores specifically in the network and adjusted by multiplying by 1000 (Orlando et al., 2013; Covani et al., 2008; Bragazzi et al., 2011; Giacomelli and Nicolini, 2006), to obtain a single score, named a weighted number of links (WNL). The total interaction score (TIS) represents all gene interactions in the entire STRING database. To obtain the TIS value, all gene interactions in the whole STRING database were summed and adjusted by multiplying by 1000. Genes with no interactions were defined as orphan genes (Orlando et al., 2013; Poswar Fde et al., 2015; Santos et al., 2017; Poswar et al., 2017; Bragazzi et al., 2011; Sobrinho-Santos et al., 2016). Based on the WNL and TIS values (Doglioni et al., 2003; Guimaraes et al., 2016a,b) a heat map was build and plotted in Microsoft Excel (Version 2016, Microsoft, Redmond, WA, USA).

2.8. Topological and ontological analyses

This study was complemented by biological systems analyses (topological and ontological analysis). The topological analyses was carried out on Cytoscape (Shannon et al., 2003), and the ontological analyses performed with BinGO (Covani et al., 2008; Giacomelli and Nicolini, 2006; Sobrinho-Santos et al., 2016; Maere et al., 2005). These analyses aid in the biological interpretation of gene interactions identified in this study, pointing to the possible molecular pathways in which gene interaction networks are involved (Santos et al., 2017).

2.9. Kyoto encyclopedia of genes and genomes (KEGG) pathways

In the KEGG database, biological pathways are described in KEGG Markup Language (KGML) files, including nodes (genes or compounds) and edges (functional links) (Kanehisa et al., 2002). The KGML data files were obtained manually from the KEGG website on 10th August, 2016.

2.10. Statistical analyses

All data have been analyzed using the software GraphPad Prism 5.0® (San Diego, USA) and submitted to specific tests with a statistical confidence of 95% ($p < .05$). The statistical significance of differences in mean values between mice groups was assessed by one-way ANOVA and the Bonferroni post hoc test. Data from the insulin sensitivity and glucose tolerance tests were evaluated by two-way ANOVA. Using the values of WNL and TIS for each related gene, the following clustering procedure was carried out using SPSS (version 18.0; IBM, New York, NY, USA). We first used K-means clustering, then validated the results with ANOVA and Tukey-Kramer post hoc test, with a P-value of < 0.001 considered statistically significant. The genes with the highest rank of associations were identified as leader genes (Poswar Fde et al., 2015; Santos et al., 2017).

3. Results

3.1. Liraglutide treatment attenuates insulin resistance and improved the lipid profile in HFD fed mice

We assessed the effects of liraglutide in body weight and adipose tissue mass. The analyses showed reduced white adipose tissue mass in

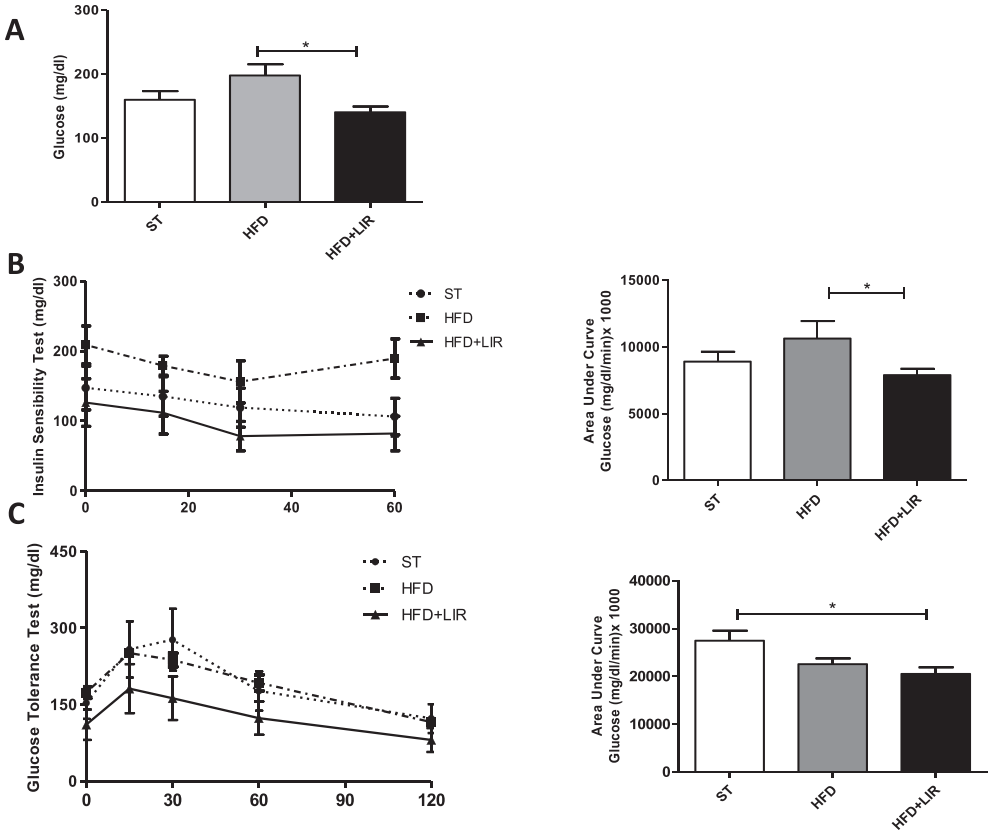

Fig. 2. Insulin sensitivity and glucose tolerance tests in mice-fed standard (ST), high-fat diet (HFD) and HFD plus liraglutide (HFD + LIR). (A) Fasting Glucose (mg/dL) (B) Intraperitoneal Insulin Sensitivity Test (IPIST) and IPIST insulin area under the curve (mg/dL) (C) Intraperitoneal glucose tolerance test (IPGTT) and IPGTT glucose area under the curve. *p < .05; **p < .01 (Two-way ANOVA).

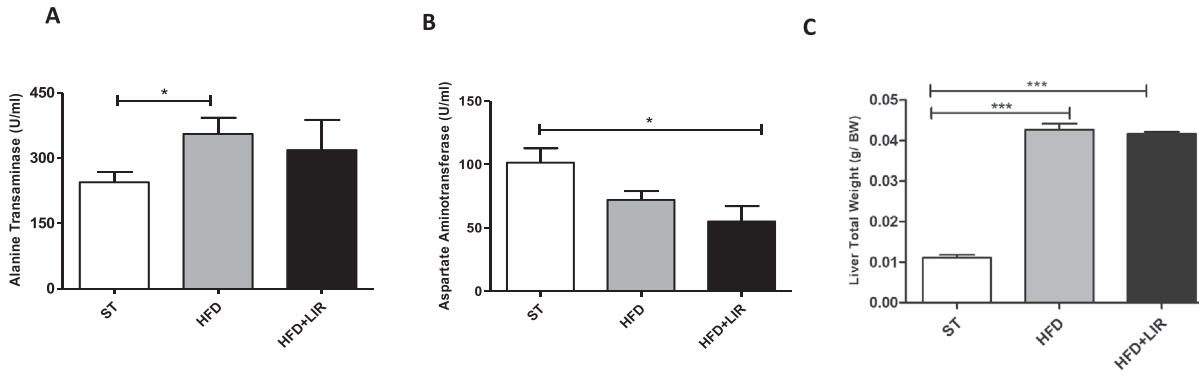

Fig. 3. Hepatic blood parameters. Hepatic function analyses showed that AST serum levels were lower in HFD + LIR as compared to the ST group, while ALT were lower to the HFD group. Control mice (white bars), mice fed a high-fat diet (HFD; gray bars), and mice liraglutide (Lir)–supplemented HFD (HFD+ LIR; black bars) for 8 weeks. *P < .05, ***P < .001 between HFD vs HFD+ LIR) and standard diet (ST). (A) ALT. (B) AST. (C) Liver total weight. *p < .05, ***p < .0001 between HFD versus ST and HFD + LIR. (For interpretation of the references to color in this figure legend, the reader is referred to the web version of this article.)

the HFD + LIR group. However, no difference was found in body weight between groups (Fig. 1A–B, supplementary data). Differences in the liver weight were not between HFD and HFD + LIR animals.

First, we evaluated the effects of the treatment with liraglutide at a biochemical level (lipid and glycemic profiles). The levels of triglycerides and total cholesterol decreased in the HFD + LIR group as compared to HFD (Fig. 1A–C). We observed a slight increase in the HDL-c levels of the HFD + LIR group, but no statistical significance association with the other groups were displayed (Fig. 1B).

The basal glycemic levels were lower in the HFD + LIR group as compared to the HFD group (Fig. 2A). Data from the Glucose tolerance test (shown on Fig. 2B) and the insulin sensitivity test (shown on Fig. 2C) are shown in Fig. 1B-C. Mice from the HFD-fed group had significantly higher glucose levels as compared to HFD + LIR.

The plasma glucose levels increase was significantly suppressed in those treated with liraglutide. The glucose area under the curve (AUC) graphs, based on the IPIST and IPGTT, showed that an eight-week drug treatment decreased the AUC of glucose in treated mice.

3.2. Effect of Liraglutide in hepatic function and on the development of fatty liver

Hepatic function analyses evidenced that aspartate aminotransferase serum levels were lower in HFD + LIR as compared to the ST group. Serum alanine transaminase levels were lower in HFD + LIR as compared to the HFD group, although no statistically significant differences were found between groups (Fig. 3A–B). The assessment of total liver weight showed no significant differences between HFD and HFD + LIR (Fig. 3C).

Histological analyzes were performed to examine the liraglutide

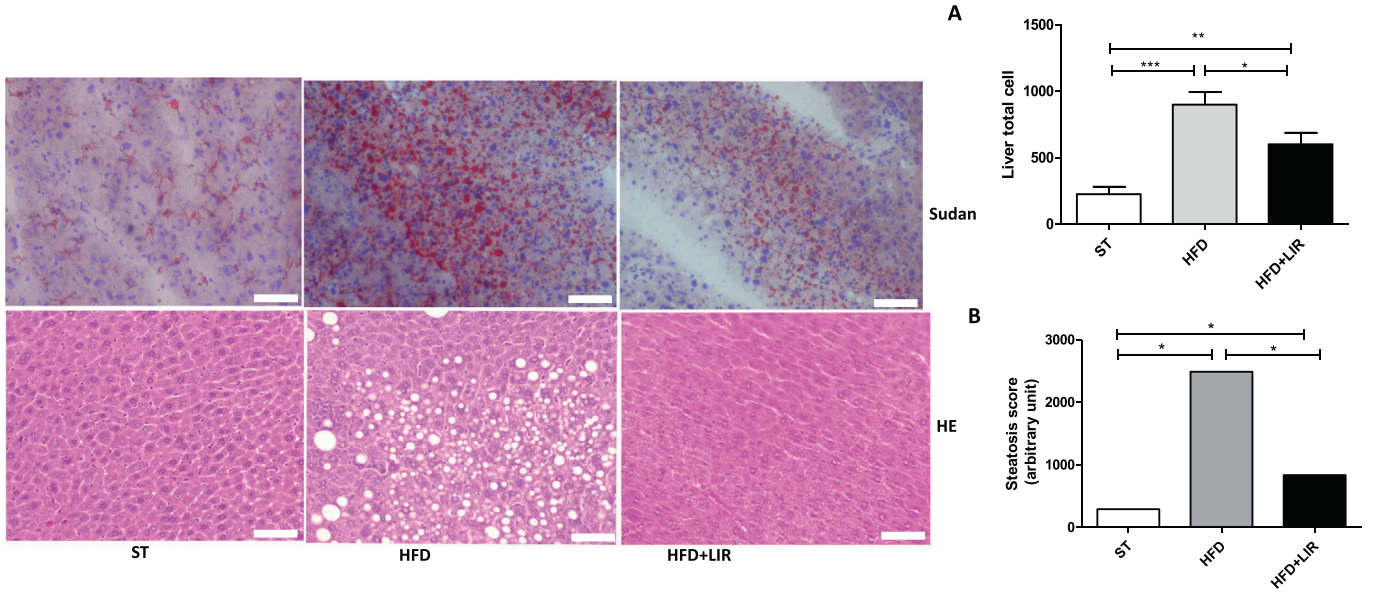

Fig. 4. Liver histological analyses stained with sudan and H&E. (A) Sudan: staining and Liver total cell. (B) Hematoxylin and eosin (HE) staining and Steatosis score. Scale bar, 50 μm. Control mice (white bars), mice fed a high-fat diet (HFD; gray bars), and mice fed liraglutide (Lir)–supplemented HFD (HFD + LIR; black bars) for 8 weeks and standard diet (ST). *p < .05, **p < .01, ***p < .0001 between HFD versus ST and HFD + LIR.

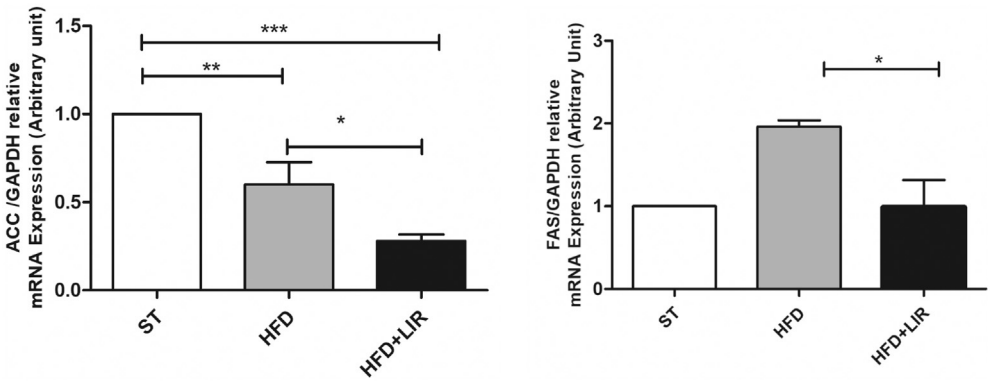

Fig. 5. ACC and FAS mRNA levels expression. Effects of 8-week liraglutide treatment on the expression levels of genes associated to the lipid metabolism in the liver of mice-fed standard (ST), high-fat diet (HFD), HFD plus liraglutide (HFD + LIR). (A) Acetyl-CoA carboxylase (ACC) (B) Fatty Acid Synthase (FAS). *p < .05; ** p < .01 (one-way ANOVA).

Table 1
Genes and their molecular functions showing WNL for each gene in the condition "Liraglutide, Obesity, glycemia, steatosis".

Gene name	Official name	Protein primary function in STRING	WNL
INS	Insulin	Insulin decreases blood glucose concentration. It increases cell permeability to monosaccharides.	29,378
GCG	Glucagon	Glicentin may modulate gastric acid secretion and the gastro-pyloro-duodenal activity. May play an important role in intestinal mucosal growth in the early period of life	10,015
ADIPOQ	Adiponectin, C1Q and collagen domain containing	Important adipokine involved in the control of fat metabolism and insulin sensitivity, with direct anti-diabetic, anti-atherogenic and anti-inflammatory activities.	3836
TNF	Tumor necrosis factor		1868
APOB	Apolipoprotein B		1804
CRP	C– reactive protein, pentraxin related	Displays several functions associated with host defense	1000
IGF1	Insulin-like growth factor 1 (Somatomedin C)	The insulin-like growth factors, isolated from plasma, are structurally and functionally related to insulin but have a much higher growth-promoting activity	21,404
SREBF1	Sterol regulatory element binding transcription factor 1	Transcriptional activator required for lipid homeostasis. Regulates transcription of the LDL receptor gene as well as the fatty acid and to a lesser degree the cholesterol synthesis pathway	12,594
LMNA	Lamin A/C		1000
ALB	Albumin		6474
KCNJ11	Potassium channel, inwardly rectifying subfamily J, member 11	This receptor is controlled by G proteins.	1000
INSR	Insulin receptor	Receptor tyrosine kinase which mediates the pleiotropic actions of insulin. Binding of insulin leads to phosphorylation of several intracellular substrates, including, insulin receptor substrates (IRS1, 2, 3, 4), SHC, GAB1, CBL and other signaling intermediates	1000

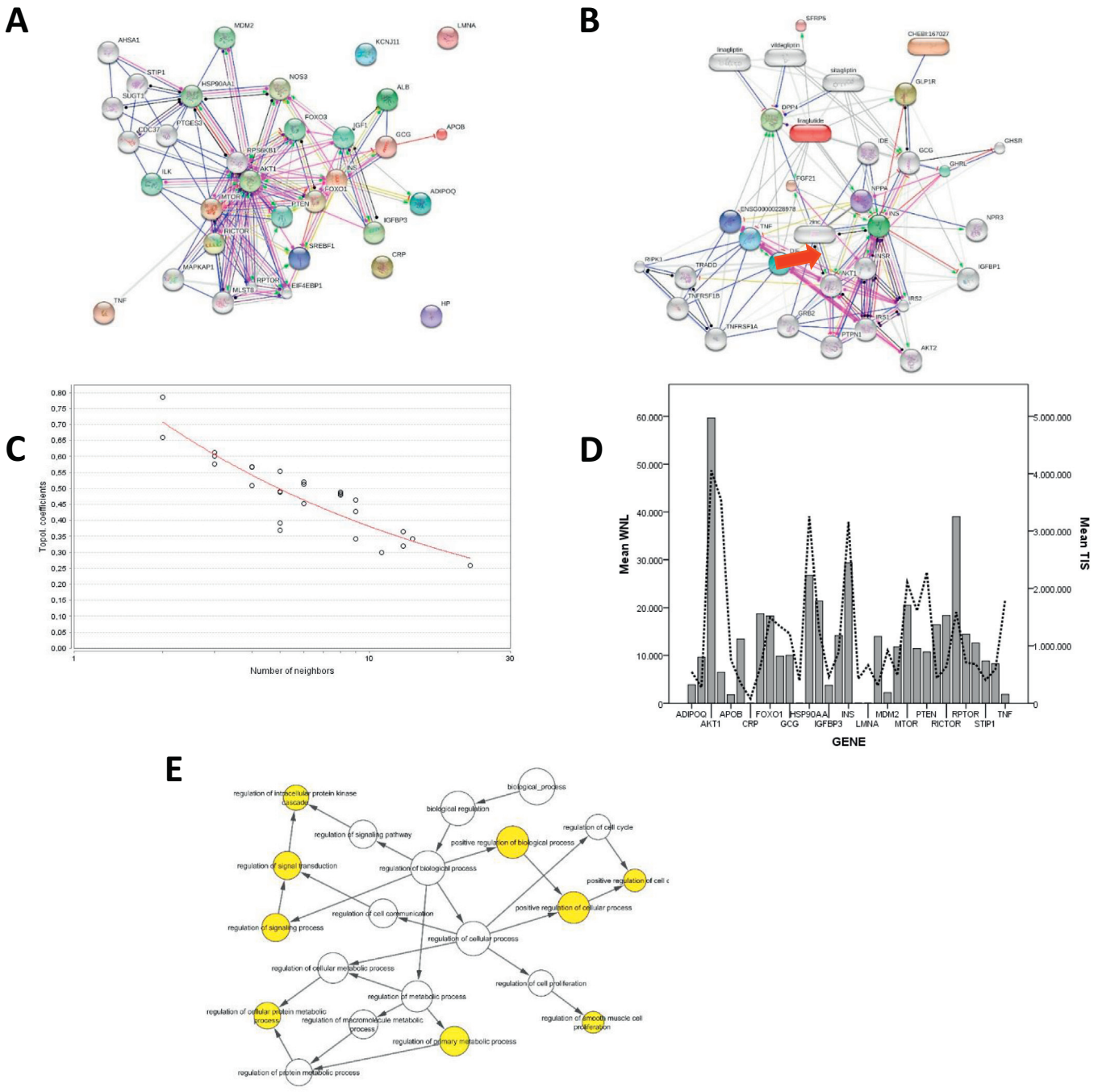

Fig. 6. Gene interaction network model. (A) The network model of interactions between genes/protein belonging to "liraglutide, liver, steatosis, and high-fat diet" subnetworks was developed by using the STRING 10 database resource search tool, under a confidence score of 0.900. (B) Interactions network between Liraglutide and protein showing its action possibilities with AKT by STITCH (C) Topological coefficients of the network. (D) Relationship between WNL and TIS means. The genes with the higher WNL and TIS values were chosen as leader genes (E) Onthologic analysis (Biological processes) showing the most important pathways over-represented in the graph versus whole set annotation, carried out with BinGO software (p-value < .0001, Benjamini-Hochberg correction. (F) The heat map, in the green area represents higher WNL and lower TIS. (For interpretation of the references to color in this figure legend, the reader is referred to the web version of this article.)

effects on the fatty liver development. The histological analyses performed with Sudan black and H&E, based on the lipid vesicle size, showed that macrovesicular standard steatosis is more prevalent among the treated groups, and regarding the steatosis classification level, the ST group was classified with normal hepatic tissue; the HFD was classified as moderate hepatic steatosis and the HFD + LIR classified as mild hepatic steatosis (Fig. 4A–B).

3.3. Effects of Liraglutide on the expression of genes ACC and FAS

We analyzed the mRNA levels expression of lipid metabolism related genes by real-time quantitative qPCR (Fig. 5A–B). Both groups ST and HFD showed increased expressions of *ACC* and *FAS* when compared to the HFD + LIR group. As expected, the treatment with liraglutide reduced the expression of these markers.

Gene	WNL	TIS
AKT1	59617	4055302
RPS6KB1	39007	1588804
INS	29378	3154044
HSP90AA	26750	3258180
IGF1	21404	1276888
MTOR	20488	2104418
EIF4EBP	18718	623972
RICTOR	18354	642676
FOXO1	18258	1492240
PTGES3	16429	436442
RPTOR	14431	710070
ILK	14159	890572
MAPKAP1	13980	305336
CDC37	13449	346566
SREBF1	12594	682478
MLST8	11794	487966
NOS3	11457	1610798
PTEN	10702	2285316
GCG	10015	1213878
FOXO3	9825	1343990
AHSA1	9649	274996
STIP1	8826	406386
SUGT1	8272	593238
ALB	6474	3543204
ADIPOQ	3836	549112
IGFBP3	3750	465376
MDM2	2235	917514
TNF	1868	1806484
APOB	1804	763500
CRP	0	80302
HP	0	393828
KCNJ11	0	426834
LMNA	0	663116

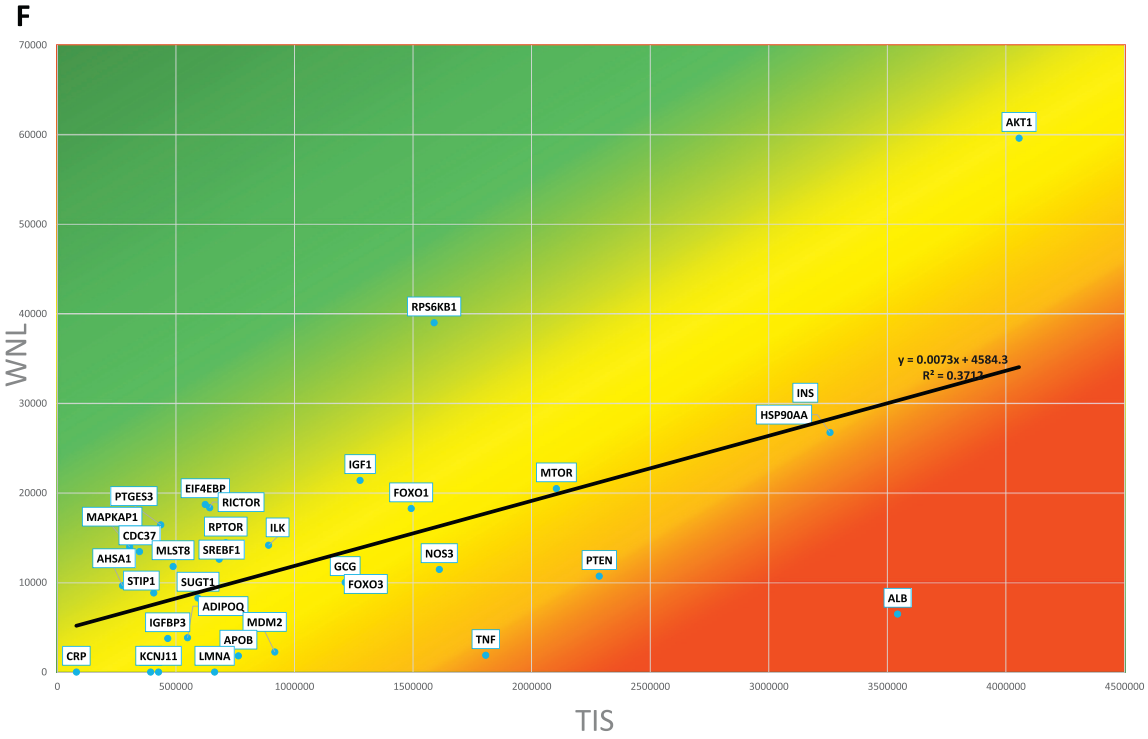

Fig. 6. (*continued*)

3.4. Bioinformatic analysis reveals the leader genes potentially modulated by Liraglutide in disorders associated with obesity, glycemia and steatosis

Following the initial search by means of several integrated experiment cross-databases, 12 genes listed by genecards were obtained, comprising the preliminary list, similar genes were also found in NCBI PubMed (Table 1. Supplementary date).

After three expansion-filtering loops, convergence was found, and the final list consisted of 31 genes. The STRING (Fig. 6A) showed the map of interactions and up and down regulation of proteins for the present phenomenon. Analyzes obtained from STITCH also guided our actions in choosing the genes to be evaluated in this study with the liraglutide drug (Fig. 6B). The network exhibited a power-law behavior (correlation: 0.891; R2:0. 776) in agreement with the scale-free theory of networks (Fig. 6C). The genes with the higher WNL and TIS values were chosen as leader genes *Serine/Threonine Kinase 1* (*AKT1*) and codes Ribosomal protein S6 kinase beta-1 (*RPS6KB1 or S6K1*) (Fig. 6D). For the analyzed process presented on the heat map, were considered as leader genes (*AKT1* and *RPS6KB1*), the others were above the trend line (Fig. 6F).

Our topological analyzes suggested that leader genes are possibly important in the biological condition “Liraglutide, Obesity, glycemia and steatosis”. The results of the ontological analyses obtained via Cytoscape and BINGO for the cluster of the leader genes approach demonstrated the overall set of cluster genes, with the respective protein number, description and involved gene (Table 2) (Fig. 6E).

3.5. Leader genes

The ‘leader genes’ were *AKT1* and *RPS6KB1*, also known as *p70S6 kinase* (*p70S6K* or *S6K1*), while some genes protrude in the scatter diagrams showing connectivity to the condition with *INS*, *AKT1*. Fig. 6F presents the overall set of cluster genes, with the respective gene number, acronyms, official names and the primary function as reported by STRING.

The Fig. 7 summarizes the the action of liraglutide on the GLP1R receptor in the liver lipogenesis pathway.

4. Discussion

The present study evaluated the metabolic effects produced by liraglutide, a GLP-1 analog, on a mice experimental model of metabolic stress induced by high-fat diet. Mice treated with a high-fat diet presented accelerated metabolic disorders development and the liraglutide treatment was able to improve some alterations.

The main findings of the current study indicated that the administration of liraglutide might inhibit hepatic lipid accumulation and alleviate hepatocyte injury by reducing aspartate aminotransferase enzyme and hepatic triglycerides stores in obese mice. Compared with previous reports, our results showed that liraglutide significantly improved total cholesterol, triglycerides levels, glucose tolerance and insulin sensitivity, but does not affect body weight. Methodological differences of the described studies, such as animal model, diet, treatment period and routes of administration can explain the mechanisms anti-obesity not observed.

Our results were corroborated by Petit et al. that demonstrated biochemical parameters improvement in patients with type 2 diabetes treated with liraglutide (Petit et al., 2016). In animal models, liraglutide was capable to prevent insulin resistance (Noyan-Ashraf et al., 2013) and reduced triglycerides, cholesterol and ALT enzyme levels in mice fed with different dietary compositions (Gao et al., 2015).

A study performed by Mells et al. (Mells et al., 2012), showed that liraglutide is capable to ameliorate hepatic steatosis without reducing body weight in obese mice. GLP-1 is one incretin, peptide hormone, that act via receptors on pancreatic β-cells, and regulates glucose homeostasis via modulation of glucagon secretion, appetite and gastric emptying (Drucker, 2006). Although several studies revealed obesity and non-alcoholic fatty liver disease protective effects of liraglutide, this drug is actually only recommended to type 2 diabetes treatment (Ao et al., 2016; Noyan-Ashraf et al., 2013).

The present data revealed molecular mechanisms that, at least in part, explain the signal effectors of liraglutide and its potential role in hepatic TG reduction. We hypothesize that liraglutide protects the damage caused by hepatic steatosis. Nonetheless, bioinformatics analyzes revealed that the mechanism involved in this process is by the

Table 2
Ontological analysis of the resulting of condition "liraglutide, liver, steatosis, and high-fat diet" network showing the significant pathways represented biological processes and the pathologic phenomenon.

Protein number	Description	*p*-Val	corr,p-val	Gene
48518	Positive regulation of biological process	1,02E-07	1,42E-04	SREBF1,HSP90AA1,NOS3,IGFBP3,ADIPOQ,PTEN,ILK,IGF1,FOXO3,TNF,FOXO1,MTOR,INS,RPTOR,RPS6KB1,MLST8, EIF4EBP1,MDM2,AKT1,RICTOR,APOB
48522	Positive regulation of cellular process	2,19E-07	1,53E-04	SREBF1,HSP90AA1,IGFBP3,ADIPOQ,PTEN, ILK,IGF1 FOXO3,TNF,FOXO1,MTOR,INS,RPTOR, RPS6KB1,MLST8, EIF4EBP1,MDM2,AKT1,RICTOR,APOB
9966	Regulation of signal transduction	5,86E-07	1,98E-04	IGFBP3,ADIPOQ,PTEN,ILK,IGF1,TNF, FOXO1,MTOR,INS, RPTOR,CDC37,MLST8,AKT1,RICTOR
23051	Regulation of signaling process	6,39E-07	1,98E-04	IGFBP3,ADIPOQ,PTEN,ILK,IGF1,TNF, FOXO1,MTOR,INS, RPTOR,CDC37,MLST8,AKT1,RICTOR
45787	Positive regulation of cell cycle	7,08E-07	1,98E-04	RPS6KB1,EIF4EBP1,MDM2,AKT1,IGF1,TNF,INS
48660	Regulation of smooth muscle cell proliferation	2,68E-06	6,23E-04	RPS6KB1,NOS3,IGFBP3,ILK,IGF1,TNF
32268	Regulation of cell protein metabolic process	3,19E-06	6,36E-04	RPS6KB1,NOS3,IGFBP3,ADIPOQ,PTEN, EIF4EBP1,MDM2, AKT1,IGF1,TNF,MTOR,INS
10627	Regulation of inteacellelar protein kinase cascade	4,11E-06	7,17E-04	ADIPOQ,PTEN,ILK,AKT1,RICTOR,IGF1,TNF,FOXO1,MTOR, INS
10646	Regulation of cell communication	9,61E-06	1,49E-03	IGFBP3,ADIPOQ,PTEN,ILK,IGF1,TNF, FOXO1,MTOR,INS, RPTOR,CDC37,MLST8,MDM2,AKT1, RICTOR
51246	Regulation of protein metabolic process	1,37E-05	1,91E-03	RPS6KB1,NOS3,IGFBP3,ADIPOQ,PTEN, EIF4EBP1,MDM2, AKT1,IGF1,TNF,MTOR,INS
43066	Negative regulation of apoptosis	1,79E-05	2,12E-03	RPS6KB1,NOS3,ALB,PTEN,ILK,AKT1,IGF1,TNF,FOXO1,INS
35466	Regulation of signaling pathway	1,82E-05	2,12E-03	ADIPOQ,PTEN,ILK,IGF1,TNF,FOXO1,MTOR,INS,RPTOR, CDC37,MLST8,MDM2,AKT1,RICTOR
43069	Negative regulation of programmed cell death	2,04E-05	2,19E-03	RPS6KB1,NOS3,ALB,PTEN,ILK,AKT1,IGF1,TNF,FOXO1,INS
9967	Positive regulation of signal transduction	2,32E-05	2,32E-03	RPTOR,ADIPOQ,MLST8,ILK,RICTOR,IGF1, TNF,MTOR,INS
60548	Negative regulationof cell death	2,49E-05	2,32E-03	RPS6KB1,NOS3,ALB,PTEN,ILK,AKT1,IGF1,TNF,FOXO1,INS
23056	Positive regulation of signalng process	2,72E-05	2,38E-03	RPTOR,ADIPOQ,MLST8,ILK,RICTOR,IGF1, TNF,MTOR,INS
42981	Regulation of apoptosis	3,02E-05	2,48E-03	NOS3,IGFBP3,ADIPOQ,PTEN,ILK,IGF1,FOXO3,TNF,FOXO1,INS,RPS6KB1,ALB,AKT1
43067	Regulation of programmed cell death	3,38E-05	2,61E-03	NOS3,IGFBP3,ADIPOQ,PTEN,ILK,IGF1,FOXO3,TNF,FOXO1,INS,RPS6KB1,ALB,AKT1
51128	Regulation of cell component organization	3,60E-05	2,61E-03	ADIPOQ,PTEN,MLST8,EIF4EBP1,ILK,AKT1,RICTOR,IGF1, TNF,MTOR,INS
10941	Regulation of cell death	3,73E-05	2,61E-03	NOS3,IGFBP3,ADIPOQ,PTEN,ILK,IGF1,FOXO3,TNF,FOXO1,INS,RPS6KB1,ALB,AKT1
51896	Regulation of protein kinase B signalng cascade	4,62E-05	3,07E-03	PTEN,ILK,RICTOR,MTOR,INS
9725	Response to hormone stimulus	8,30E-05	5,27E-03	RPS6KB1,NOS3,ADIPOQ,PTEN,EIF4EBP1,AKT1,GCG,TNF, FOXO1,MTOR
51726	Regulation of cell cycle	9,24E-05	5,61E-03	RPS6KB1,CDC37,PTEN,EIF4EBP1,MDM2, ILK,AKT1,IGF1, TNF,INS
10906	Regulation of glucose metabolic process	9,92E-05	5,78E-03	ADIPOQ,AKT1,IGF1,MTOR,INS
50793	Regulation of developmental process	1,63E-04	9,12E-03	RPS6KB1,NOS3,IGFBP3,ADIPOQ,PTEN,ILK,AKT1,IGF1, FOXO3,APOB,TNF,INS
51094	Positive regulation of developmental process	1,71E-04	9,20E-03	RPS6KB1,NOS3,IGFBP3,ILK,AKT1,FOXO3, APOB,TNF,INS
10608	Postranscriptional regulation of gene expression	1,83E-04	9,46E-03	RPS6KB1,NOS3,PTEN,EIF4EBP1,MDM2,AKT1,TNF,MTOR
31667	Response to nutrient levels	1,95E-04	9,72E-03	RPTOR,SREBF1,RPS6KB1,ADIPOQ,ALB, PTEN,AKT1,MTOR

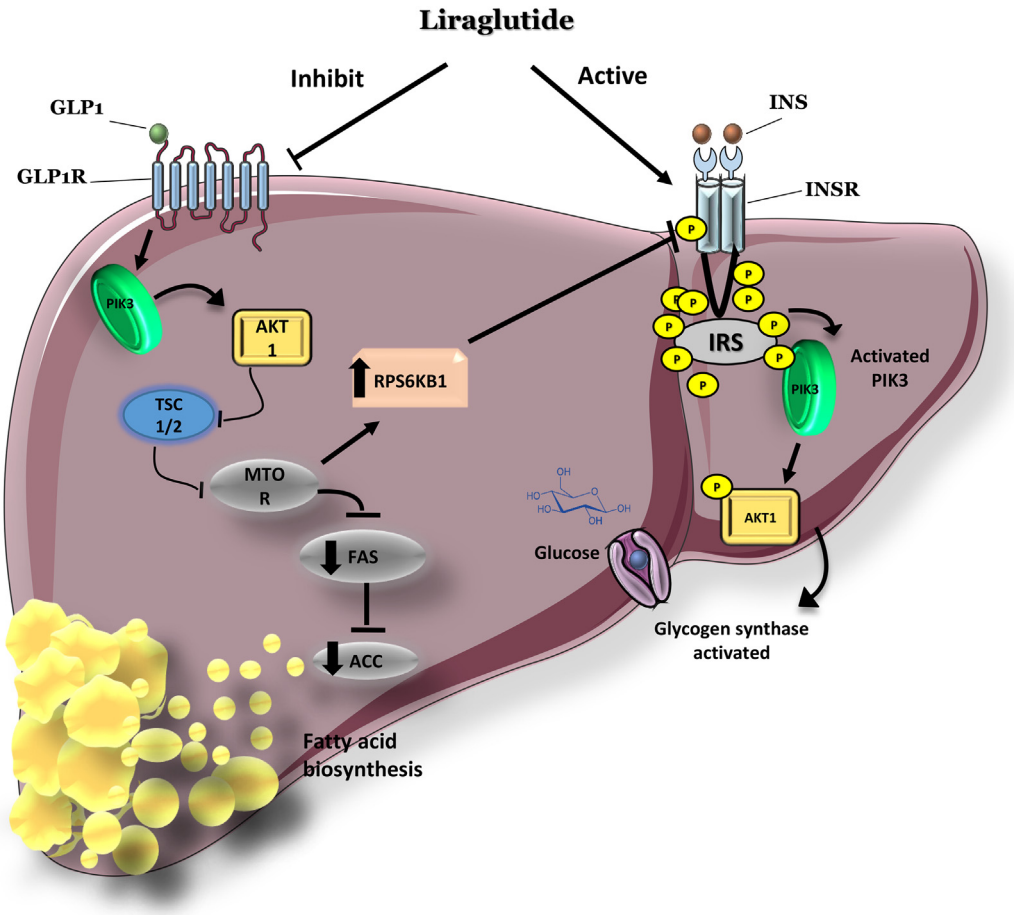

Fig. 7. Illustrative pathway fig. A model illustrating how Liraglutide fits within the INS/Akt signaling network. Insulin or insulin-like growth factor initiates signaling at the insulin receptor, leading to activation of IRS1 and PI3KR5. The lipid products of PI3K, PIP3 (i.e. phosphatidylinositol 3,4,5 trisphosphate and phosphatidylinositol 3,4 bisphosphate), recruit Akt to the plasma membrane, stimulating glycogen synthase activated. When GLP/Akt then phosphorylates numerous targets to promote growth and survival, including the TSC1/2 complex. By phosphorylating TSC2, Akt inactivates TSC2s. mTORC1 phosphorylates several targets, including the translation control proteins S6K inactivates INSR stimulating fatty acid biosynthesis.

regulation of *AKT* and *S6K1* expression, considered GLP-1 targets in hepatic steatosis, which under high-fat diet treatment, acts by favoring the obesity development and consequently hepatic steatosis.

Other studies has demonstrated that GLP-1, produced in enteroendocrine cells in the distal small bowel and colon, and receptor expressed in kidney, lung and heart, also exerts indirect actions in other cell types, as hepatocytes and muscle (Drucker, 2006; Panjwani et al., 2013). GLP-1 is rapidly eliminated from the circulation by activation of dipeptidyl peptidase-4 (DPP4), considered the principal enzyme responsible for GLP-1 inactivation (Flock et al., 2007).

Based on our data and using bioinformatics analyzes we have outlined a proposed molecular pathway whereby GLP-1 or homologs intersect the insulin signaling pathway in hepatocytes (Fig. 5), since this and inter-related pathways has emerged as critical for the hepatocyte insulin resistance molecular basis.

GLP-1, a glucose-dependent incretin, exerts its beneficial effects by increasing fatty acid oxidation, improving insulin resistance and decreasing lipogenesis (Koo, 2013; Postic and Girard, 2008). When NAFLD occurs, excess *FAS* in the liver cells lead to the lipogenesis increase and the generation of a large number of adipocytes (Koo, 2013). Consequently, these processes inhibit mitochondria respiration and induces and aggravates insulin resistance (Nieto-Vazquez et al., 2008; Polyzos et al., 2009). This study has clearly revealed that targeting *ACC* has beneficial effects on both hepatic steatosis and insulin resistance, and that treatment with liraglutide promoted a decrease in the expression of transcription factors and genes regulating fatty acid synthesis in *ACC* and *FAS* signaling, the enzymes involved in fatty acid synthesis (Morgan et al., 2008).

Insulin resistance is an important contributing factor of hepatic diseases, characterized by a reduced phosphorylation kinase activity in the receptor signaling protein (*IRS)* 1 and 2 and glucose translocation transporters (GLUTs) (Pessin and Saltiel, 2000). In a study by Sajan et al. (2009), with *IRS-1* and 2 knockout rat hepatocytes, they appear to activate the *AKT* pathway (Sajan et al., 2009), considered a key effector for insulin signaling. It has been widely reported that *AKT* phosphorylation is markedly diminished in hepatic steatosis (Piro et al., 2008).

Based on the main findings of the present study, it appears that more than one pathway related to insulin signal transduction, and a decrease in the hepatocytes TG content were modulated by GLP-1 proteins. Here we show through the bioinformatics analyses that GLP-1 ligands regulated not only the *AKT* phosphorylation status, but other downstream key molecules, such as *S6K1* (Noyan-Ashraf et al., 2013; Pessin and Saltiel, 2000; Sajan et al., 2009).

Published studies demonstrated that the glucagon-like peptide 1 (GLP-1) and its cognate receptor GLP-1R are present in human hepatocytes (Gupta et al., 2010). The expression of GLP-1R in hepatocytes is still controversial. Flock and collaborates, did not observe direct effects of GLP-1 on cholesterol or TG synthesis or secretion in isolated murine hepatocytes, although significant changes in the levels of hepatic enzymes were seen (Flock et al., 2007). GLP-1R mRNA transcripts have not been detected in RNA from isolated murine hepatocytes, reducing indirectly hepatic lipid accumulation (Panjwani et al., 2013). siRNA

studies knocking out the GLP-1R demonstrate a novel insulin action of GLP-1 proteins by up regulating hepatocyte insulin signaling pathway key elements (Sajan et al., 2009). These data suggest that, in addition to its pancreatic properties, GLP-1 analogs have direct insulin-sensitizing effects in hepatocytes.

Quinn and Birnbaum (2012) identify that *Akt,* mTORC1 and *S6K1* are key components of the insulin pathway, by promoting de novo lipogenesis (Quinn 3rd and Birnbaum, 2012). The protein kinase mTORC phosphorylates and activates *S6K1*, which regulates several fundamental cellular processes, including transcription, protein translation and synthesis and cell metabolism. In vitro, mTORC1 signaling can cause cell intrinsic insulin resistance through negative feedback mechanisms affecting *Akt* upstream regulators (Dibble et al., 2009; Harrington et al., 2005). Elevated mTORC1 levels have been associated to hepatic insulin resistance (Noyan-Ashraf et al., 2013; Pessin and Saltiel, 2000; Sajan et al., 2009).

Interestingly, this study identified by bioinformatics analyses, the role of *S6K1* gene, as a leader gene in hepatic steatosis. Our literature search revealed a study where pathways that involve the mTOR and *S6K1* expression ameliorates liver steatosis in livers of db/db mice, which are a genetic model of obesity, through the transcription cofactor (BTG1) (Xiao et al., 2016).

Recent studies with *S6K1* knockout mouse have demonstrated the anti-obesity effects of *S6K1* in adiposity, hyperinsulinemia and glucose intolerance (Briggs et al., 2003; Fingar et al., 2002; Pende et al., 2000). In high-fat fed *S6K1*-deficient mice, glucose and free fatty acids are increased, resulting in insulin receptor desensitization (Um et al., 2004). Furthermore, another study showed that *S6K1*-deficient mice maintain normal glucose levels during fasting, suggesting hypersensitivity to insulin (Pende et al., 2000). In addition, reports have shown that *S6K1* knockout mice leads to an increased *Akt* signaling response to insulin in the liver and other metabolic tissues (Um et al., 2004).

It is important to note that the results obtained with the bioinformatics analyses are promising, but should be carefully interpreted. The browsing networks for interest genes, inspecting interaction evidence and performing interactive clustering, led to functional association networks with *Akt* and *S6K1* as leader genes (Um et al., 2004). In the scientific literature, bioinformatic studies that evaluated the interaction of genes in hepatic steatosis are inexistent, emphasizing the innovative character of this study. However, several studies aimed to explore the liraglutide mechanisms and target genes on hepatic steatosis through experimental models are described in the literature (Ono et al., 2003; Koketsu et al., 2008; Fleischmann and Iynedjian, 2000; Leavens et al., 2009; Kuang et al., 2017).

In this sense, the present study is the first to show interaction networks between protein-coding genes, leader genes and molecular pathways using bioinformatics analyzes that can be related to hepatic steatosis pathogenesis associated with liraglutide treatment. The TIS is associated with extensive interactions while WNL is related to specific network interactions (Poswar et al., 2017). The use of combined WNL and TIS values for the gene clustering is critical to identify targets genes, as the WNL values for gene clustering might be a confusion factor, since genes with higher TIS values act in several biological process (Poswar et al., 2017).

In conclusion, we showed that a 2-month treatment with liraglutide improves metabolic conditions and induces a significant liver fat content decrease in high-fat fed obese mice. Our results contribute to a better understanding of the hepatoprotective effects of liraglutide and give subsidies for the therapeutic potential of this pharmacologic compound in the hepatic steatosis treatment. However, taking into account the limitations of the present study, future cellular analyzes should focus on GLP-1 proteins as insulin sensitizing agents in hepatocytes, to elucidate the liraglutide effects on liver metabolism.

Acknowledgements

This work was partially supported by grants from the Coordenadoria de Aperfeiçoamento do Pessoal de Nível Superior (CAPES), Conselho Nacional de Desenvolvimento Científico e Tecnológico (CNPq), and Fundação de Amparo à Pesquisa de Minas Gerais (FAPEMIG).

Appendix A. Supplementary data

Supplementary data to this article can be found online at https://doi.org/10.1016/j.mgene.2019.100553.

References

Ao, N., Yang, J., Wang, X., Du, J., 2016. Glucagon-like peptide-1 preserves non-alcoholic fatty liver disease through inhibition of the endoplasmic reticulum stress-associated pathway. Hepatol. Res. 46 (4), 343–353.
Bambha, K., Belt, P., Abraham, M., Wilson, L.A., Pabst, M., Ferrell, L., et al., 2012. Ethnicity and nonalcoholic fatty liver disease. Hepatology (Baltimore, Md) 55 (3), 769–780.
Bode, B., 2012. An overview of the pharmacokinetics, efficacy and safety of liraglutide. Diabetes Res. Clin. Pract. 97 (1), 27–42.
Bragazzi, N.L., Sivozhelezov, V., Nicolini, C., 2011. LeaderGene: a fast data-mining tool for molecular genomics. J. Proteomics Bioinform. 04, 201.
Briggs, J.A., Wilk, T., Welker, R., Krausslich, H.G., Fuller, S.D., 2003. Structural organization of authentic, mature HIV-1 virions and cores. EMBO J. 22 (7), 1707–1715.
Buettner, R., Scholmerich, J., Bollheimer, L.C., 2007. High-fat diets: modeling the metabolic disorders of human obesity in rodents. Obesity 15 (4), 798–808.
Cameron-Smith, D., Burke, L.M., Angus, D.J., Tunstall, R.J., Cox, G.R., Bonen, A., et al., 2003. A short-term, high-fat diet up-regulates lipid metabolism and gene expression in human skeletal muscle. Am. J. Clin. Nutr. 77 (2), 313–318.
Cohen, J.C., Horton, J.D., Hobbs, H.H., 2011. Human fatty liver disease: old questions and new insights. Science. 332 (6037), 1519–1523.
Covani, U., Marconcini, S., Giacomelli, L., Sivozhelevov, V., Barone, A., Nicolini, C., 2008. Bioinformatic prediction of leader genes in human periodontitis. J. Periodontol. 79 (10), 1974–1983.
Dibble, C.C., Asara, J.M., Manning, B.D., 2009. Characterization of Rictor phosphorylation sites reveals direct regulation of mTOR complex 2 by S6K1. Mol. Cell. Biol. 29 (21), 5657–5670.
Doglioni, C., Piccinin, S., Demontis, S., Cangi, M.G., Pecciarini, L., Chiarelli, C., et al., 2003. Alterations of beta-catenin pathway in non-melanoma skin tumors: loss of alpha-ABC nuclear reactivity correlates with the presence of beta-catenin gene mutation. Am. J. Pathol. 163 (6), 2277–2287.
Drucker, D.J., 2006. The biology of incretin hormones. Cell Metab. 3 (3), 153–165.
Fingar, D.C., Salama, S., Tsou, C., Harlow, E., Blenis, J., 2002. Mammalian cell size is controlled by mTOR and its downstream targets S6K1 and 4EBP1/eIF4E. Genes Dev. 16 (12), 1472–1487.
Fleischmann, M., Iynedjian, P.B., 2000. Regulation of sterol regulatory-element binding protein 1 gene expression in liver: role of insulin and protein kinase B/cAkt. Biochem. J. 349 (Pt 1), 13–17.
Flock, G., Baggio, L.L., Longuet, C., Drucker, D.J., 2007. Incretin receptors for glucagon-like peptide 1 and glucose-dependent insulinotropic polypeptide are essential for the sustained metabolic actions of vildagliptin in mice. Diabetes 56 (12), 3006–3013.
Fotbolcu, H., Zorlu, E., 2016. Nonalcoholic fatty liver disease as a multi-systemic disease. World J. Gastroenterol. 22 (16), 4079–4090.
Gao, H., Zeng, Z., Zhang, H., Zhou, X., Guan, L., Deng, W., et al., 2015. The glucagon-like peptide-1 analogue liraglutide inhibits oxidative stress and inflammatory response in the liver of rats with diet-induced non-alcoholic fatty liver disease. Biol. Pharm. Bull. 38 (5), 694–702.
Giacomelli, L., Nicolini, C., 2006. Gene expression of human T lymphocytes cell cycle: experimental and bioinformatic analysis. J. Cell. Biochem. 99 (5), 1326–1333.
Guimaraes, T.A., Farias, L.C., Fraga, C.A., Feltenberger, J.D., Melo, G.A., Coletta, R.D., et al., 2016a. Evaluation of the antineoplastic activity of gallic acid in oral squamous cell carcinoma under hypoxic conditions. Anti-Cancer Drugs 27 (5), 407–416.
Guimaraes, T.A., Farias, L.C., Santos, E.S., de Carvalho Fraga, C.A., Orsini, L.A., de Freitas, Teles L., et al., 2016b. Metformin increases PDH and suppresses HIF-1alpha under hypoxic conditions and induces cell death in oral squamous cell carcinoma. Oncotarget 7 (34), 55057–55068.
Gupta, N.A., Mells, J., Dunham, R.M., Grakoui, A., Handy, J., Saxena, N.K., et al., 2010. Glucagon-like peptide-1 receptor is present on human hepatocytes and has a direct role in decreasing hepatic steatosis in vitro by modulating elements of the insulin signaling pathway. Hepatology (Baltimore, Md) 51 (5), 1584–1592.
Harrington, L.S., Findlay, G.M., Lamb, R.F., 2005. Restraining PI3K: mTOR signaling goes back to the membrane. Trends Biochem. Sci. 30 (1), 35–42.
Jensen, L.J., Kuhn, M., Stark, M., Chaffron, S., Creevey, C., Muller, J., et al., 2009. STRING 8–a global view on proteins and their functional interactions in 630 organisms. Nucleic Acids Res. 37 (Database issue), D412–D416.
Kanehisa, M., Goto, S., Kawashima, S., Nakaya, A., 2002. The KEGG databases at GenomeNet. Nucleic Acids Res. 30 (1), 42–46.
Kim, W., Egan, J.M., 2008. The role of incretins in glucose homeostasis and diabetes

treatment. Pharmacol. Rev. 60 (4), 470–512.
Koketsu, Y., Sakoda, H., Fujishiro, M., Kushiyama, A., Fukushima, Y., Ono, H., et al., 2008. Hepatic overexpression of a dominant negative form of raptor enhances Akt phosphorylation and restores insulin sensitivity in K/KAy mice. Am. J. Physiol. Endocrinol. Metab. 294 (4), E719–E725.
Koo, S.H., 2013. Nonalcoholic fatty liver disease: molecular mechanisms for the hepatic steatosis. Clin. Mol. Hepatol. 19 (3), 210–215.
Kuang, J.R., Zhang, Z.H., Leng, W.L., Lei, X.T., Liang, Z.W., 2017. Dapper1 attenuates hepatic gluconeogenesis and lipogenesis by activating PI3K/Akt signaling. Mol. Cell. Endocrinol. 447, 106–115.
Leavens, K.F., Easton, R.M., Shulman, G.I., Previs, S.F., Birnbaum, M.J., 2009. Akt2 is required for hepatic lipid accumulation in models of insulin resistance. Cell Metab. 10 (5), 405–418.
Lee, J., Hong, S.W., Rhee, E.J., Lee, W.Y., 2012. GLP-1 receptor agonist and non-alcoholic fatty liver disease. Diabetes Metab. J. 36 (4), 262–267.
Livak, K.J., Schmittgen, T.D., 2001. Analysis of relative gene expression data using real-time quantitative PCR and the 2(−Delta Delta C(T)) Method. Methods (San Diego, Calif) 25 (4), 402–408.
Maere, S., Heymans, K., Kuiper, M., 2005. BiNGO: a Cytoscape plugin to assess over-representation of gene ontology categories in biological networks. Bioinformatics 21 (16), 3448–3449.
Mells, J.E., Fu, P.P., Sharma, S., Olson, D., Cheng, L., Handy, J.A., et al., 2012. Glp-1 analog, liraglutide, ameliorates hepatic steatosis and cardiac hypertrophy in C57BL/6J mice fed a Western diet. Am. J. Physiol. Gastrointest. Liver Physiol. 302 (2), G225–G235.
Morgan, K., Uyuni, A., Nandgiri, G., Mao, L., Castaneda, L., Kathirvel, E., et al., 2008. Altered expression of transcription factors and genes regulating lipogenesis in liver and adipose tissue of mice with high fat diet-induced obesity and nonalcoholic fatty liver disease. Eur. J. Gastroenterol. Hepatol. 20 (9), 843–854.
Ng, S.F., Lin, R.C., Laybutt, D.R., Barres, R., Owens, J.A., Morris, M.J., 2010. Chronic high-fat diet in fathers programs beta-cell dysfunction in female rat offspring. Nature 467 (7318), 963–966.
Nieto-Vazquez, I., Fernandez-Veledo, S., Kramer, D.K., Vila-Bedmar, R., Garcia-Guerra, L., Lorenzo, M., 2008. Insulin resistance associated to obesity: the link TNF-alpha. Arch. Physiol. Biochem. 114 (3), 183–194.
Noyan-Ashraf, M.H., Shikatani, E.A., Schuiki, I., Mukovozov, I., Wu, J., Li, R.K., et al., 2013. A glucagon-like peptide-1 analog reverses the molecular pathology and cardiac dysfunction of a mouse model of obesity. Circulation 127 (1), 74–85.
Ono, H., Shimano, H., Katagiri, H., Yahagi, N., Sakoda, H., Onishi, Y., et al., 2003. Hepatic Akt activation induces marked hypoglycemia, hepatomegaly, and hypertriglyceridemia with sterol regulatory element binding protein involvement. Diabetes 52 (12), 2905–2913.
Orlando, B., Bragazzi, N., Nicolini, C., 2013. Bioinformatics and systems biology analysis of genes network involved in OLP (Oral Lichen Planus) pathogenesis. Arch. Oral Biol. 58 (6), 664–673.
Panjwani, N., Mulvihill, E.E., Longuet, C., Yusta, B., Campbell, J.E., Brown, T.J., et al., 2013. GLP-1 receptor activation indirectly reduces hepatic lipid accumulation but does not attenuate development of atherosclerosis in diabetic male ApoE(−/−) mice. Endocrinology 154 (1), 127–139.
Pende, M., Kozma, S.C., Jaquet, M., Oorschot, V., Burcelin, R., Le Marchand-Brustel, Y., et al., 2000. Hypoinsulinaemia, glucose intolerance and diminished beta-cell size in S6K1-deficient mice. Nature 408 (6815), 994–997.
Pessin, J.E., Saltiel, A.R., 2000. Signaling pathways in insulin action: molecular targets of insulin resistance. J. Clin. Invest. 106 (2), 165–169.
Petit, J.M., Cercueil, J.P., Loffroy, R., Denimal, D., Bouillet, B., Fourmont, C., et al., 2016. Effect of liraglutide therapy on liver fat content in patients with inadequately controlled type 2 diabetes. The Lira-NAFLD study. J. Clin. Endocrinol. Metabol. 102 (2), 407–415 jc20162775.
Piro, S., Spadaro, L., Russello, M., Spampinato, D., Oliveri, C.E., Vasquez, E., et al., 2008. Molecular determinants of insulin resistance, cell apoptosis and lipid accumulation in non-alcoholic steatohepatitis. Nutr. Metabol. Cardiovasc. Dis. 18 (8), 545–552.
Polyzos, S.A., Kountouras, J., Zavos, C., 2009. Nonalcoholic fatty liver disease: the pathogenetic roles of insulin resistance and adipocytokines. Curr. Mol. Med. 9 (3), 299–314.
Postic, C., Girard, J., 2008. Contribution of de novo fatty acid synthesis to hepatic steatosis and insulin resistance: lessons from genetically engineered mice. J. Clin. Invest. 118 (3), 829–838.
Poswar Fde, O., Farias, L.C., Fraga, C.A., Bambirra Jr., W., Brito-Junior, M., Sousa-Neto, M.D., et al., 2015. Bioinformatics, interaction network analysis, and neural networks to characterize gene expression of radicular cyst and periapical granuloma. J. Endod. 41 (6), 877–883.
Poswar, FdO, Santos, L.I., Farias, L.C., Guimarães, T.A., Santos, S.H.S., Jones, K.M., et al., 2017. An adaptation of particle swarm clustering applied in basal cell carcinoma, squamous cell carcinoma of the skin and actinic keratosis. Meta Gene. 12, 72–77.
Quinn 3rd, W.J., Birnbaum, M.J., 2012. Distinct mTORC1 pathways for transcription and cleavage of SREBP-1c. Proc. Natl. Acad. Sci. U. S. A. 109 (40), 15974–15975.
Rebhan, M., Chalifa-Caspi, V., Prilusky, J., Lancet, D., 1997. GeneCards: integrating information about genes, proteins and diseases. Trends Genet. 13 (4), 163.
Rector, R.S., Thyfault, J.P., Wei, Y., Ibdah, J.A., 2008. Non-alcoholic fatty liver disease and the metabolic syndrome: an update. World J. Gastroenterol. 14 (2), 185–192.
Sajan, M.P., Standaert, M.L., Nimal, S., Varanasi, U., Pastoor, T., Mastorides, S., et al., 2009. The critical role of atypical protein kinase C in activating hepatic SREBP-1c and NFkappaB in obesity. J. Lipid Res. 50 (6), 1133–1145.
Santos, E.M., Farias, L.C., Santos, S.H., de Paula, A.M., Oliveira, E.S.C.S., Guimaraes, A.L., 2017. Molecular finds of pressure ulcer: A bioinformatics approach in pressure ulcer. J. Tissue Viability 26 (2), 119–124.
Scott, L.J., 2014. Liraglutide: a review of its use in adult patients with type 2 diabetes mellitus. Drugs 74 (18), 2161–2174.
Shannon, A.M., Bouchier-Hayes, D.J., Condron, C.M., Toomey, D., 2003. Tumor hypoxia, chemotherapeutic resistance and hypoxia-related therapies. Cancer Treat. Rev. 29 (4), 297–307.
Shepard, T.Y., Weil, K.M., Sharp, T.A., Grunwald, G.K., Bell, M.L., Hill, J.O., et al., 2001. Occasional physical inactivity combined with a high-fat diet may be important in the development and maintenance of obesity in human subjects. Am. J. Clin. Nutr. 73 (4), 703–708.
Sobrinho-Santos, E.S., Dias, I., Santos, S., de Paula, A., Feltenberger, J., Guimarães, A., et al., 2016. Bioinformatics analysis reveals genes involved in the pathogenesis of ameloblastoma and keratocystic odontogenic tumor. Int. J. Mol. Cell. Med. 5 (4), 1–21.
Stal, P., 2015. Liver fibrosis in non-alcoholic fatty liver disease – diagnostic challenge with prognostic significance. World J. Gastroenterol. 21 (39), 11077–11087.
Targher, G., Marra, F., Marchesini, G., 2008. Increased risk of cardiovascular disease in non-alcoholic fatty liver disease: causal effect or epiphenomenon? Diabetologia 51 (11), 1947–1953.
Um, S.H., Frigerio, F., Watanabe, M., Picard, F., Joaquin, M., Sticker, M., et al., 2004. Absence of S6K1 protects against age- and diet-induced obesity while enhancing insulin sensitivity. Nature 431 (7005), 200–205.
von Mering, C., Jensen, L.J., Snel, B., Hooper, S.D., Krupp, M., Foglierini, M., et al., 2005. STRING: known and predicted protein-protein associations, integrated and transferred across organisms. Nucleic Acids Res. 33 (Database issue), D433–D437.
Weisberg, S.P., Hunter, D., Huber, R., Lemieux, J., Slaymaker, S., Vaddi, K., et al., 2006. CCR2 modulates inflammatory and metabolic effects of high-fat feeding. J. Clin. Invest. 116 (1), 115–124.
Xiao, F., Deng, J., Guo, Y., Niu, Y., Yuan, F., Yu, J., et al., 2016. BTG1 ameliorates liver steatosis by decreasing stearoyl-CoA desaturase 1 (SCD1) abundance and altering hepatic lipid metabolism. Sci. Signal. 9 (428), ra50.

Update

Meta Gene

Volume 30, Issue , December 2021, Page

DOI: https://doi.org/10.1016/j.mgene.2021.100919

Meta Gene 30 (2021) 100919

Contents lists available at ScienceDirect

Meta Gene

journal homepage: www.elsevier.com/locate/mgene

Erratum regarding missing Declaration of Competing Interest statements in previously published articles

Declaration of Competing Interest statements were not included in published version of the.

following articles that appeared in previous issues of Meta Gene. Hence, the authors of the below articles were contacted after publication to request a Declaration of Interest statement:

1. "Liraglutide alters hepatic metabolism in high-fat fed obese mice: A bioinformatic prediction and functional analysis" [Meta Gene, 2019; 20C: 100553] https://doi.org/10.1016/j.mgene.2019.100553
2. "A new mutation in steroidogenic acute regulatory protein (StAR) is segregated in an Iranian family" [Meta Gene, 2018; 16C: 196–198] https://doi.org/10.1016/j.mgene.2018.03.005
3. "Alteration of the risk of oral pre-cancer and cancer in North Indian population by XPC polymorphism genotypes and haplotypes" [Meta Gene, 2019; 21C: 100583] https://doi.org/10.1016/j.mgene.2019.100583
4. "Shortening the list of essential genes in the human genome by network analysis" [Meta Gene, 2018; 17C: 68–77] https://doi.org/10.1016/j.mgene.2018.05.001
5. "Spectrum of clinical manifestations of SLE patients from India and its correlation with KIR gene polymorphism" [Meta Gene, 2018; 17C: 99–107] https://doi.org/10.1016/j.mgene.2018.05.007
6. "A simulations approach for meta-analysis of genetic association studies based on additive genetic model" [Meta Gene, 2018; 16C: 143–164] https://doi.org/10.1016/j.mgene.2018.02.004
7. "Evaluation of caries experience in two genders and ENAM polymorphism in Iranian adults" [Meta Gene, 2018; 17C: 78–81] https://doi.org/10.1016/j.mgene.2018.05.002
8. "Discovering microRNAs and their targets in the red flour beetle *Tribolium castaneum* from expressed sequence tags" [Meta Gene, 2018; 17C: 61–67] https://doi.org/10.1016/j.mgene.2018.03.009

DOIs of original article: https://doi.org/10.1016/j.mgene.2019.100553, https://doi.org/10.1016/j.mgene.2018.05.007, https://doi.org/10.1016/j.mgene.2018.05.002, https://doi.org/10.1016/j.mgene.2018.03.005, https://doi.org/10.1016/j.mgene.2018.05.001, https://doi.org/10.1016/j.mgene.2019.100583, https://doi.org/10.1016/j.mgene.2018.03.009, https://doi.org/10.1016/j.mgene.2018.02.004.

https://doi.org/10.1016/j.mgene.2021.100919

Available online 3 July 2021